Progress In Electromagnetics Research M, Vol. 96, 129–138, 2020

Rigorous Quantum Formulation of Parity-Time Symmetric Coupled Resonators

Shaolin Liao[1, *] and Lu Ou[2]

Abstract—Rigorous quantum formulation of the Parity-Time (PT) symmetry phenomenon in the RF/microwave regime for a pair of coil resonators with lump elements has been presented. The coil resonator is described by the lump-element model that consists of an inductor (L), a resistor (R), and a capacitor (C). Rigorous quantum Hamiltonian for the coupled RLC coil resonators system has been derived through twice basis transforms of the original basis. The first basis transform rotates the original basis such that off-diagonal terms of the governing matrix of the equation system of the coupled coil resonators is reduced to constants. Then a second basis transform obtains the quantum Hamiltonian, including the diagonal effective complex frequencies and off-diagonal coupling terms, together with the transformed basis. With the obtained quantum Hamiltonian, the eigenvalues and eigenvectors of the coupled coil resonators can be obtained as usual as the quantum Hamiltonian. Finally, numerical simulation verifies the correctness of the theory. The quantum formulation of the coupled coil resonators can provide better guideline to design a better PT-symmetric system.

1. INTRODUCTION

Parity-Time (PT) symmetry has shown great potential as ultra-sensitive sensors [1, 2], Wireless Power Transfer (WPT [3–5]), gain/loss controlled lasers [6], and absorber [7], in both the photonics [8, 9] and microwave [10] regimes. PT symmetry is a physics phenomenon that originates from the quantum community: it was first proposed in quantum mechanics by Bender and Boettcher in 1998 [11]. Counterintuitively, it is argued that real eigenfequencies exist even for a non-Hermitian Hamiltonian when a quantum system is invariant under operations of spatial reflection $\mathcal{P}(x)$ and time reversal $\mathcal{T}(t)$ operations. This can be made clear by looking at the Hamiltonian given below [12],

$$\mathcal{H}(\omega) = \begin{bmatrix} \Omega - jg & 1 \\ 1 & \Omega + jg \end{bmatrix}, \tag{1}$$

where the Hamiltonian has been normalized by the diagonal coupling strength κ; Ω is the normalized natural frequency of the two identical coupled resonators; $\pm g$ are the normalized gain/loss of the coupled resonators. The eigenfrequencies of the Hamiltonian in Eq. (1) are given by,

$$\Omega_{\pm} = \Omega \pm \sqrt{1 - g^2}, \tag{2}$$

from which it can be seen that the eigenfequencies are real when the gain/loss is smaller than the coupling strength, i.e., $g < 1$ and are imaginary when the gain/loss is larger than the coupling strength, i.e., $g > 1$; finally, when the gain/loss is equal to the coupling strength, i.e., $g = 1$, the two eigenfrequencies coalesce to an identical eigenfrequency, which is called the Exception Point (EP).

Received 26 June 2020, Accepted 3 September 2020, Scheduled 17 September 2020

* Corresponding author: Shaolin Liao (sliao5@iit.edu).

[1] Department of Electrical and Computer Engineering, Illinois Institute of Technology, Chicago, IL 60616, USA. [2] College of Computer Science and Electronic Engineering, Hunan University, Changsha, Hunan 410082, China.

The existence of PT-symmetric quantum system has not been experimentally demonstrated due to the difficulty of generating the non-Hermitian quantum system. However, gain and loss can be readily introduced in photonics [13–20]. So PT symmetry can be introduced by designing the proper gain-loss profile so that the PT symmetry phenomenon happens. Following the pioneering theoretical work by El-Ganainy et al. [21], the feasibility of translating this quantum-inspired symmetry to the optics regime has been demonstrated in a various contributions and, specifically, in coupled optical structures [22–27]. Later, it has also been demonstrated in the electromagnetic and acoustic systems [28, 29], whose governing Helmholtz equation [30–47] is similar to the Schrödinger equation in the quantum physics. These PT-symmetric wave systems are usually realized by introducing the spatial distribution of balanced gain-loss profiles.

In particular, at RF and microwave frequencies, a PT-symmetric system can be readily realized with transmission-line networks or lumped-element circuits [48–51]. However, most of the works above take the quantum Hamiltonian as granted, assuming that the diagonal natural frequencies are the resonant frequencies of the coupled coil resonators and that the off-diagonal coupling terms are known. Also, it is generally assumed that the basis of the quantum Hamiltonian consists of stored energies in the coupled coil resonators, but no clear formula exists. In this paper, rigorous quantum formulation has been derived, and all of these will be clear, providing guideline to design a better coupled coil resonators and its system [1, 52, 53].

2. THE COUPLED RLC COIL RESONATORS

A resonant coil can be modeled as an RLC tank that consists of 3 components in parallel: an inductor with inductance L, a capacitor with capacitance C, and a resistor R. The RLC tank in series can be converted to the RLC tank in parallel through the Kirchhoff Voltage Law (KVL) and Kirchhoff Current Law (KCL).

2.1. The Governing Equations System

When a pair of RLC resonant tanks are brought close to each other, they are coupled together through magnetic flux of the two inductive coils, which can be characterized by the mutual inductance M. The coupled resonant coils can be analyzed by the physical quantities of currents i_1/i_2 and voltages v_1/v_2 through the indicators of the two coupled coil resonators,

$$v_1 = L_1\frac{di_1}{dt} + M\frac{di_2}{dt}, \quad v_2 = L_2\frac{di_2}{dt} + M\frac{di_1}{dt}. \tag{3}$$

The Kirchhoff Current Law (KCL) connects the currents through the inductor with inductance L, the capacitor with capacitance C, and the resistor with conductance G as follows,

$$i_1 + C_1\frac{dv_1}{dt} + G_1v_1 = 0, \quad i_2 + C_2\frac{dv_2}{dt} + G_2v_2 = 0. \tag{4}$$

Taking Fourier transforms on Eq. (3) and Eq. (4), after some mathematics, the following is obtained,

$$\begin{aligned}\left(\frac{-\omega^2}{\omega_1^2} + \frac{j\omega}{\alpha_1} + 1\right)v_1(\omega) + \left(\frac{-\omega^2}{\kappa_2^2} + \frac{j\omega}{\gamma_2}\right)v_2(\omega) = 0\\ \left(\frac{-\omega^2}{\omega_2^2} + \frac{j\omega}{\alpha_2} + 1\right)v_2(\omega) + \left(\frac{-\omega^2}{\kappa_1^2} + \frac{j\omega}{\gamma_1}\right)v_1(\omega) = 0,\end{aligned} \tag{5}$$

with

$$\begin{aligned}\omega_1 &= \frac{1}{\sqrt{L_1C_1}}, \quad \alpha_1 = \frac{1}{L_1G_1}, \quad \kappa_1 = \frac{1}{\sqrt{MC_1}}, \quad \gamma_1 = \frac{1}{MG_1},\\ \omega_2 &= \frac{1}{\sqrt{L_2C_2}}, \quad \alpha_2 = \frac{1}{L_2G_2}, \quad \kappa_2 = \frac{1}{\sqrt{MC_2}}, \quad \gamma_2 = \frac{1}{MG_2}.\end{aligned}$$

Equation (5) can be normalized by scaling the frequency $\tilde{\omega} = \omega/\omega_1$ as follows,

$$\begin{aligned} \left(-\tilde{\omega}^2 + \frac{j\tilde{\omega}}{\tilde{\alpha}_1} + 1\right) v_1(\tilde{\omega}) + \left(\frac{-\tilde{\omega}^2}{\tilde{\kappa}_2^2} + \frac{j\tilde{\omega}}{\tilde{\gamma}_2}\right) v_2(\tilde{\omega}) = 0, \\ \left(\frac{-\tilde{\omega}^2}{\tilde{\omega}_2^2} + \frac{j\tilde{\omega}}{\tilde{\alpha}_2} + 1\right) v_2(\tilde{\omega}) + \left(\frac{-\tilde{\omega}^2}{\tilde{\kappa}_1^2} + \frac{j\tilde{\omega}}{\tilde{\gamma}_1}\right) v_1(\tilde{\omega}) = 0, \end{aligned} \tag{6}$$

with

$$\begin{aligned} \tilde{\alpha}_1 &= \frac{1}{\tilde{G}_1}, \quad \tilde{\kappa}_1 = \frac{1}{\sqrt{\tilde{M}}}, \quad \gamma_1 = \frac{1}{\tilde{M}\tilde{G}_1}, \\ \tilde{\omega}_2 &= \frac{1}{\sqrt{\tilde{L}_2\tilde{C}_2}}, \quad \tilde{\alpha}_2 = \frac{1}{\tilde{L}_2\tilde{G}_2}, \quad \tilde{\kappa}_2 = \frac{1}{\sqrt{\tilde{M}\tilde{C}_2}}, \quad \gamma_2 = \frac{1}{\tilde{M}\tilde{G}_2}, \end{aligned}$$

and the normalized quantities defined below,

$$\begin{aligned} \tilde{G}_1 &= \sqrt{\frac{L_1}{C_1}} G_1, \quad \tilde{M} = \frac{M}{L_1}, \\ \tilde{L}_2 &= \frac{L_2}{L_1}, \quad \tilde{C}_2 = \frac{C_2}{C_1}, \quad \tilde{G}_2 = \sqrt{\frac{L_1}{C_1}} G_2. \end{aligned}$$

In terms of matrix form, Eq. (6) can be expressed as follows,

$$\overline{\overline{M}}(\tilde{\omega}) \begin{bmatrix} v_1(\tilde{\omega}) \\ v_2(\tilde{\omega}) \end{bmatrix} = 0, \tag{7}$$

with

$$\overline{\overline{M}}(\tilde{\omega}) = \begin{bmatrix} -\tilde{\omega}^2 + \frac{j\tilde{\omega}}{\tilde{\alpha}_1} + 1 & \frac{-\tilde{\omega}^2}{\tilde{\kappa}_2^2} + \frac{j\tilde{\omega}}{\tilde{\gamma}_2} \\ \frac{-\tilde{\omega}^2}{\tilde{\kappa}_1^2} + \frac{j\tilde{\omega}}{\tilde{\gamma}_1} & \frac{-\tilde{\omega}^2}{\tilde{\omega}_2^2} + \frac{j\tilde{\omega}}{\tilde{\alpha}_2} + 1 \end{bmatrix}.$$

2.2. The Hamiltonian of the Coupled RLC Coil Resonators

From Eq. (7), it can be seen that matrix equations contain second order frequency components. To cast the matrix equation into the Hamiltonian of a coupled resonators, two times of changes of basis are required.

During the first basis change, $\overline{\overline{M}}(\tilde{\omega})$ is transformed such that the diagonal terms are reduced to zeros, and the following transformation matrix $\overline{\overline{T}}_1$ is given below,

$$\overline{\overline{T}}_1 = \begin{bmatrix} L_2 & -M \\ -M & L_1 \end{bmatrix}. \tag{8}$$

Then a second change of basis is performed with the transformation matrix $\overline{\overline{T}}_2$, and the Hamiltonian equations of the coupled resonators can be expressed as follows,

$$\overline{\overline{T}}_1 \overline{\overline{M}}(\tilde{\omega}) \begin{bmatrix} v_1(\tilde{\omega}) \\ v_2(\tilde{\omega}) \end{bmatrix} = \left[\tilde{\omega}\overline{\overline{I}} - \mathcal{H}(\tilde{\omega})\right] \overline{\overline{T}}_2 \begin{bmatrix} v_1(\tilde{\omega}) \\ v_2(\tilde{\omega}) \end{bmatrix} = 0, \tag{9}$$

where $\overline{\overline{I}}$ is the unit matrix and

$$\mathcal{H}(\tilde{\omega}) = \begin{bmatrix} \tilde{\Omega}_1 & \kappa_{1,2} \\ \kappa_{2,1} & \tilde{\Omega}_2 \end{bmatrix}, \tag{10}$$

and the following transformation matrix,

$$\overline{\overline{T}}_2 = \begin{bmatrix} \tilde{\omega} - \tilde{\Omega}_1' & \kappa_{1,2}' \\ \kappa_{2,1}' & \tilde{\omega} - \tilde{\Omega}_2' \end{bmatrix}. \tag{11}$$

Substituting Eq. (11) into Eq. (9), the following is obtained,

$$\overline{\overline{T}}_1 \overline{\overline{M}}(\tilde{\omega}) = \left[\tilde{\omega}\overline{\overline{I}} - \mathcal{H}(\tilde{\omega})\right] \overline{\overline{T}}_2, \tag{12}$$

from which all the unknown parameters can be solved.

2.3. The Eigenvalues and Eigenvectors

With the obtained Hamiltonian $\mathcal{H}$, the eigenvalues of the coupled resonant coils are given by,

$$\tilde{\Omega}^{\pm} = \frac{\tilde{\Omega}_1 + \tilde{\Omega}_2}{2} \pm \sqrt{\kappa_{12}\kappa_{21} + \left(\frac{\tilde{\Omega}_1 - \tilde{\Omega}_2}{2}\right)^2}, \tag{13}$$

and the corresponding eigenvectors are as follows,

$$v^{\pm} = \left[\frac{\kappa_{12}}{\tilde{\Omega}^{\pm} - \tilde{\Omega}_1}, 1\right]^T. \tag{14}$$

2.4. Solutions of the Hamiltonian

The solution of the Hamiltonian $\mathcal{H}$ and the corresponding basis transform matrix $\overline{\overline{U}}$ can be obtained by solving Eq. (12), which are shown as follows,

$$\tilde{\Omega}_1^{\pm} = j\frac{G_1}{2} \pm \tilde{\Omega}\left(\tilde{\Omega}_2^{\pm}\right), \tag{15}$$

with

$$\left\{\left[\tilde{\Omega}\left(\tilde{\Omega}_2^{\pm}\right)\right]^2 - \Gamma^2\right\}\left\{\left[\tilde{\Omega}^{\pm}\left(\tilde{\Omega}_2^{\pm}\right)\right]^2 - \Gamma'^2\right\} + M^2 = 0,$$

and the following parameters,

$$\begin{aligned}
\tilde{\Omega}\left(\tilde{\Omega}_2^{\pm}\right) &= \sqrt{\left(\tilde{\Omega}_2^{\pm} - j\frac{G_2}{2C_2}\right)^2 + (\Gamma^2 - \Lambda^2)}, \\
\tilde{\Omega}^{\pm}\left(\tilde{\Omega}_2^{\pm}\right) &= \tilde{\Omega}_2^{\pm} \pm \tilde{\Omega}\left(\tilde{\Omega}_2^{\pm}\right) - j\frac{G_2}{2C_2}, \\
\Lambda &= \frac{1}{2C_2}\sqrt{\frac{4C_2 - G_2^2L_2 + G_2^2M^2}{L_2 - M^2}} \\
\Gamma &= \frac{1}{2}\sqrt{\frac{4L_2 - G_1^2L_2 + G_1^2M^2}{L_2 - M^2}}, \quad \Gamma' = j\left(\frac{G_2}{2C_2} - \frac{G_1}{2}\right).
\end{aligned}$$

Also, the coupling terms κ_{12} and κ_{21} are obtained as follows,

$$\kappa_{12} = \frac{M}{-j\frac{G_2}{C_2} + \tilde{\Omega}_1 + \tilde{\Omega}_2}; \quad \kappa_{21} = \frac{\Gamma^2 - \left(\tilde{\Omega}_1 - j\frac{G_1}{2}\right)^2}{\kappa_{12}}. \tag{16}$$

Finally, other parameters such as $\tilde{\Omega}_1', \tilde{\Omega}_2', \kappa_{12}', \kappa_{21}'$ of the transformation matrix $\overline{\overline{T}}_2$ can be obtained accordingly.

$$\begin{aligned}
&\tilde{\Omega}_1'^{\pm} = jG_1 - \tilde{\Omega}_1^{\pm}, \quad \tilde{\Omega}_2'^{\pm} = \frac{C_2M}{jG_2 - C_2\tilde{\Omega}_1^{\pm} - C_2\tilde{\Omega}_2^{\pm}}, \\
&\kappa_{12}' = c_3\tilde{\Omega}_1^{\pm 3} + c_2\tilde{\Omega}_1^{\pm 2} + c_1\tilde{\Omega}_1^{\pm} + c_0, \quad \kappa_{21}' = \tilde{\Omega}_2^{\pm} - j\frac{G_2}{C_2},
\end{aligned} \tag{17}$$

with

$$\begin{aligned}
c_1 &= \frac{jG_1\tilde{\Omega}_2^{\pm}}{M} + \frac{L_2}{M(L_2 - M^2)} + \frac{G_1G_2}{C_2M}, \\
c_2 &= -\frac{\tilde{\Omega}_2^{\pm}}{M} + j\left(\frac{G_1}{M} + \frac{G_2}{C_2M}\right), \\
c_3 &= -\frac{1}{M}, \quad c_0 = L_2\frac{C_2\tilde{\Omega}_2^{\pm} - jG_2}{C_2M(L_2 - M^2)}.
\end{aligned}$$

3. DISCUSSION

Analytical solutions exist for some special cases. Also, the Hamiltonian can be normalized to give the unit frequency of one coil resonator, i.e., $\omega_1 = 1$.

3.1. Identical Resonant Frequencies and Decay Rates

When the two resonant coils have identical resonant frequencies and decay rates, the following is satisfied,

$$\omega_1 = \frac{1}{\sqrt{L_1 C_1}} = \omega_2 = \frac{1}{\sqrt{L_2 C_2}}; \quad \tau_1 = \frac{G_1}{C_1} = \tau_2 = \frac{G_2}{C_2},$$

from which Eq. (15) has the following four solutions,

$$\tilde{\Omega}_1 = \tilde{\Omega}_2 = \pm \frac{\sqrt{\Gamma^2 \pm \sqrt{-M^2 + \Gamma^4}}}{\sqrt{2}} + j\frac{G_1}{2}.$$

3.2. Parity-Time Symmetry

When the loss and gain of the resonant coils balance each other, the following is satisfied,

$$\omega_1 = \frac{1}{\sqrt{L_1 C_1}} = \omega_2 = \frac{1}{\sqrt{L_2 C_2}}; \quad \tau_1 = \frac{G_1}{C_1} = \tau_2 = -\frac{G_2}{C_2},$$

from which Eq. (15) has the following six solutions,

$$\tilde{\Omega}_1 = -\tilde{\Omega}_2 = j\left(\frac{G_1}{2} \pm \frac{\sqrt{M^2 - G_1^2\Gamma^2}}{G_1}\right), \tag{18}$$

and

$$\begin{aligned} \tilde{\Omega}_1 &= \tilde{\Omega}_2 + jG_1, \\ \tilde{\Omega}_2 &= \pm \frac{\sqrt{\Gamma^2 - \frac{G_1^2}{4} \pm \sqrt{-M^2 + \left(\Gamma^2 + \frac{G_1^2}{4}\right)^2}}}{\sqrt{2}} - j\frac{G_1}{2}. \end{aligned}$$

3.3. Identical Lossless Resonators Frequencies

When the two resonant coils have identical resonant frequencies and lossless,

$$\omega_1 = \frac{1}{\sqrt{L_1 C_1}} = \omega_2 = \frac{1}{\sqrt{L_2 C_2}}; \quad G_1 = G_2 = 0,$$

and the following solutions are obtained,

$$\tilde{\Omega}_1 = \tilde{\Omega}_2 = \pm\sqrt{\frac{L_2 \pm \sqrt{L_2^2 - M^2(M^2 - L_2)^2}}{2(L_2 - M^2)}}, \tag{19}$$

and

$$\kappa_{12} = \kappa_{21} = \frac{M}{2\tilde{\Omega}_1},$$

which gives the the eigenvalues and eigenvectors according to Eq. (13) and Eq. (14) as follows,

$$\tilde{\Omega}^{\pm} = \tilde{\Omega}_1 \pm \kappa_{12}, \quad v^{\pm} = [\pm 1, 1]^T, \tag{20}$$

agreeing with symmetric/anti-symmetric eigenmodes due to the off-diagonal coupling.

3.4. Applications

The derived rigorous eigenfrequencies and eigenvectors have many potential applications. For example, to design an optimal dynamic WPT system [4] where the Hamiltonian of the coupled PT resonant coils changes with time, rigorous eigenvectors that change with time can be used to achieve the optimal adiabatic PT WPT system.

4. SIMULATION RESULTS

Numerical simulation with Python has been performed to confirm the correctness of the quantum formulation. Simulation results of two typical cases are shown here: 1) identical resonant frequencies and decay rates case as shown in Section 3.1; and 2) PT symmetry case as shown in Section 3.2.

Figure 1 shows the surface and contours plots for case 1) with $\omega_1 = 1/\sqrt{L_1C_1} = \omega_2 = 1/\sqrt{L_2C_2} = 1$ and $G_1 = G_2$: a) real part of the mean of the two eigenfrequencies, i.e., $\Re\{\overline{\tilde{\Omega}}\} = (\Re\{\tilde{\Omega^+}\} + \Re\{\tilde{\Omega^-})/2\}$; b) imaginary part of the mean of the two eigenfrequencies, i.e., $\Im\{\overline{\tilde{\Omega}}\} = (\Im\{\tilde{\Omega^+}\} + \Im\{\tilde{\Omega^-})/2\}$; c) deviation of real part of one eigenfrequency from the real part of the two eigenfrequencies' mean, i.e., $\Re\{\tilde{\Omega}^+\} - \Re\{\overline{\tilde{\Omega}}\}$; and d) deviation of real part of the other eigenfrequency from the real part of the two eigenfrequencies' mean, i.e., $\Re\{\tilde{\Omega}^-\} - \Re\{\overline{\tilde{\Omega}}\}$. Fig. 1(a) shows that the two eigenfrequencies' mean value increases for an increasing coupling coefficient M. Also, Fig. 1(b) shows an increasing imaginary part of the mean eigenfrequency when the losses of the coil resonators $G_1 = G_2$ increase. Note that

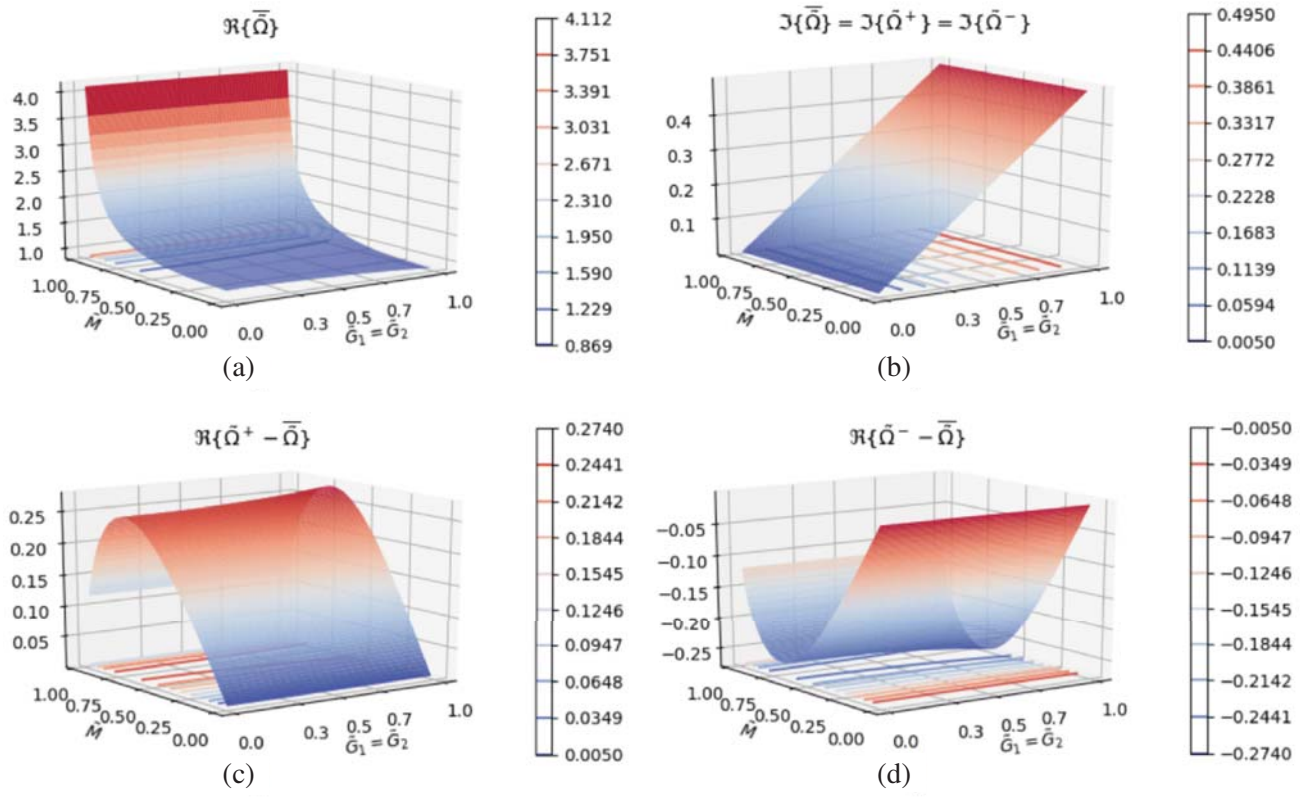

Figure 1. Simulation result for the coupled coil resonators pair with identical resonant frequencies and decay rates: (a) the real part of the mean of the two eigenfrequencies; (b) the imaginary part of the mean of the two eigenfrequencies; (c) the deviation of the real part of eigenfrequency #1 from the real part of the eigenfrequency mean; and (d) the deviation of the real part of eigenfrequency #2 from the real part of the eigenfrequency mean.

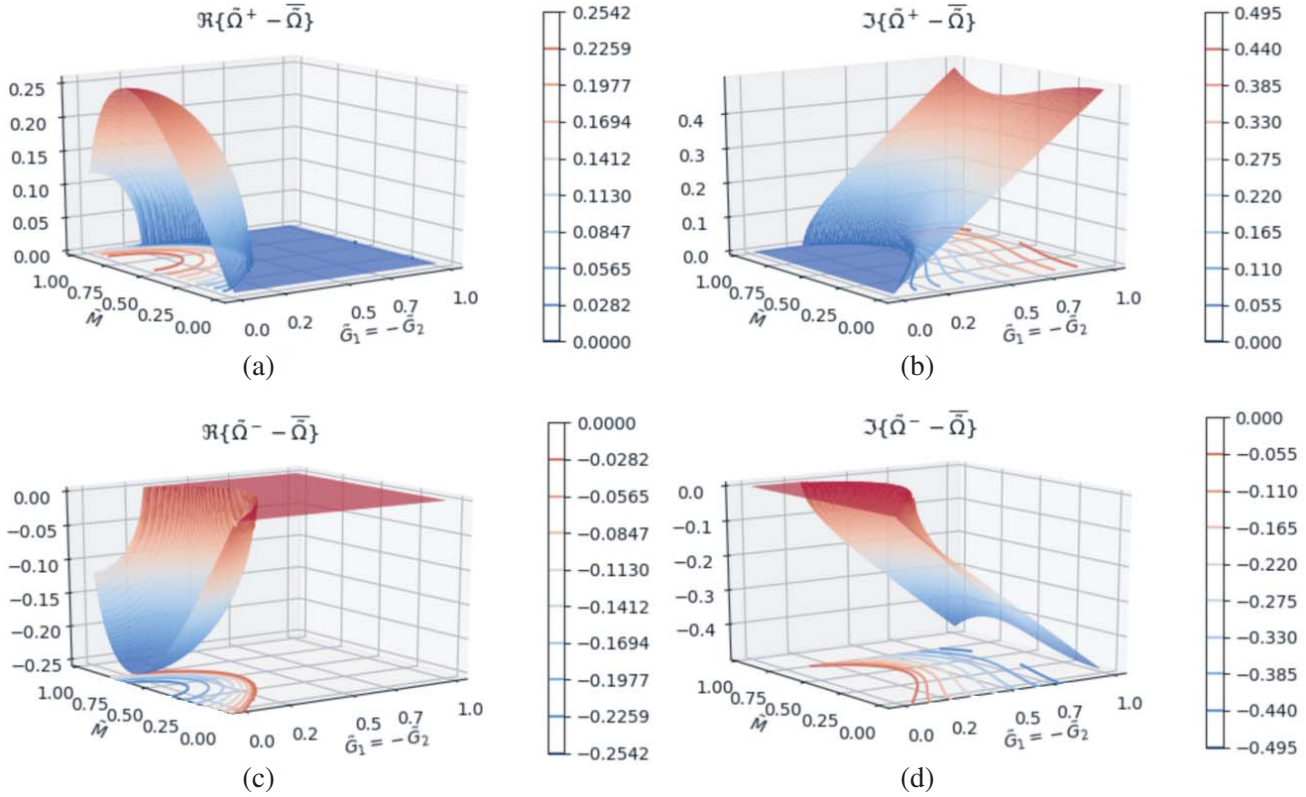

Figure 2. Simulation result for the PT-symmetric coupled resonator pair with balanced gain and loss: (a) the deviation of the real part of eigenfrequency #1 from the eigenfrequency mean; (b) the deviation of the imaginary part of eigenfrequency #1 from the eigenfrequency mean; (c) the deviation of the real part of eigenfrequency #2 from the eigenfrequency mean; (d) the deviation of the imaginary part of eigenfrequency #2 from the eigenfrequency mean.

the imaginary parts of the two eigenfrequencies are identical due to symmetry. Finally, Fig. 1(c) and Fig. 1(d) show the deviation of the real parts of the two eigenfrequencies from that of the eigenfrequency mean: it is clear that the deviations are anti-symmetric due to symmetry and repelling coupling effect.

Figure 2 shows the surface and contour plots for PT-symmetry case 2) with $\omega_1 = 1/\sqrt{L_1C_1} = \omega_2 = 1/\sqrt{L_2C_2} = 1$ and $G_1 = -G_2$: a) deviation of the real part of the eigenfrequency #1 from that of the eigenfrequency mean, i.e., $\Re\{\tilde{\Omega}^+\} - \Re\{\overline{\tilde{\Omega}}\}$; b) deviation of the imaginary part of the eigenfrequency #1 from that of the eigenfrequency mean, i.e., $\Im\{\tilde{\Omega}^+\} - \Im\{\overline{\tilde{\Omega}}\}$; c) deviation of the real part of the eigenfrequency #2 from that of the eigenfrequency mean, i.e., $\Re\{\tilde{\Omega}^-\} - \Re\{\overline{\tilde{\Omega}}\}$; and d) deviation of the imaginary part of the eigenfrequency #2 from that of the eigenfrequency mean, i.e., $\Im\{\tilde{\Omega}^-\} - \Im\{\overline{\tilde{\Omega}}\}$. Comparing Fig. 2(a) to Fig. 2(c), and Fig. 2(b) to Fig. 2(d), it is clear that the deviation of both the real part and imaginary part of the eigenfrequencies is anti-symmetric, due to the anti-symmetry of the PT-symmetric gain/loss profile. More importantly, Fig. 2(a) to Fig. 2(d) clearly show the evolution of the real eigenfrequencies to the imaginary eigenfrequencies when the gain/loss $G_1 = -G_2$ becomes larger than the coupling coefficient M, confirming the EPs of the PT-symmetric system. At last, when the gain/loss is large enough, no real eigenfrequencies exist for such non-Hermitian Hamiltonian system.

5. CONCLUSION

Quantum formulation of the PT symmetric coupled RLC coil resonators system has been derived. Starting from the governing equation system, two basis transforms are performed to transform the

second order frequencies equations system in the frequency domain to a quantum Hamiltonian and the corresponding new basis. The first basis transform is to make off-diagonal terms of the equations system to be constant values that contain no frequency term. Then a second basis transform is performed to obtain the quantum Hamiltonian with the off-diagonal effective complex frequencies and the off-diagonal coupling terms, together with the new basis that denotes the coupled quantum states. With the obtained quantum Hamiltonian, eigenvalues and the corresponding eigenvectors can be obtained as usual. Finally, numerical simulation confirms the correctness of the theory. It is expected that the quantum formulation of the coupled coil resonators provides helpful insight and guideline for the PT symmetric RF/microwave resonators and systems. Potential applications include the design of an optimal dynamic PT WPT system.

ACKNOWLEDGMENT

The work is partly supported by China Postdoctoral Science Foundation No. 2020M672488.

REFERENCES

1. Hajizadegan, M., M. Sakhdari, S. Liao, and P. Chen, "High-sensitivity wireless displacement sensing enabled by PT-symmetric telemetry," *IEEE Transactions on Antennas and Propagation*, Vol. 67, No. 5, 3445–3449, May 2019.
2. Sakhdari, M., M. Hajizadegan, Y. Li, M. M. Cheng, J. C. H. Hung, and P. Chen, "Ultrasensitive, parity-time-symmetric wireless reactive and resistive sensors," *IEEE Sensors Journal*, Vol. 18, No. 23, 9548–9555, December 2018.
3. Assawaworrarit, S. and S. Fan, "Robust and efficient wireless power transfer using a switch-mode implementation of a nonlinear parity-time symmetric circuit," *Nature Electronics*, Vol. 3, 273–279, 2020.
4. Paul, K. and A. K. Sarma, "Fast and efficient wireless power transfer via transitionless quantum driving," *Scientific Reports*, Vol. 8, Article number: 4134, March 2018.
5. Assawaworrarit, S., X. Yu, and S. Fan, "Robust wireless power transfer using a nonlinear parity-time-symmetric circuit," *Nature*, Vol. 546, No. 7658, 387–390, June 2017.
6. Gao, Z., S. T. M. Fryslie, B. J. Thompson, P. S. Carney, and K. D. Choquette, "Parity-time symmetry in coherently coupled vertical cavity laser arrays," *Optica*, Vol. 4, No. 3, 323–329, March 2017.
7. Wang, H., W. Kong, P. Zhang, Z. Li, and D. Zhong, "Coherent perfect absorption laser points in one-dimensional anti-parity-time-symmetric photonic crystals," *Applied Sciences*, Vol. 9, No. 13, 2738, January 2019.
8. Phang, S., A. Vukovic, S. C. Creagh, P. D. Sewell, G. Gradoni, and T. M. Benson, "Localized single frequency lasing states in a finite parity-time symmetric resonator chain," *Scientific Reports*, Vol. 6, 20499, February 2016.
9. Cui, X., K. Ding, J.-W. Dong, and C. T. Chan, "Exceptional points and their coalescence of PT-symmetric interface states in photonic crystals," *Physical Review B*, Vol. 100, No. 11, 115412, September 2019.
10. Liu, Y., T. Hao, W. Li, J. Capmany, N. Zhu, and M. Li, "Observation of parity-time symmetry in microwave photonics," *Light: Science & Applications*, Vol. 7, No. 1, 1–9, July 2018.
11. Bender, C. M. and S. Boettcher, "Real spectra in non-hermitian hamiltonians having PT symmetry," *Physical Review Letters*, Vol. 80, No. 24, 5243–5246, June 1998.
12. Özdemir, Ş. K., S. Rotter, F. Nori, and L. Yang, "Parity–time symmetry and exceptional points in photonics," *Nature Materials*, Vol. 18, 783–798, 2019.
13. Liao, S., T. Wong, and L. Ou, "Optimal feedback-interferometric fiber laser microphones," *Optics Letters*, Vol. 45, No. 2, 423–426, Optical Society of America, January 2020.
14. Liao, S., "Optimal feedback-interferometric fiber laser sensors," *2019 Photonics & Electromagnetics Research Symposium —Fall (PIERS — Fall)*, Xiamen, China, December 17–20, 2019.

15. Liao, S. and T. Wong, "Optimal design of feedback-interferometric fiber laser sensors," *IEEE Sensors Journal*, Vol. 19, No. 24, 12016–12023, December 2019.
16. Peng, Y. and S. Liao, "ZIM laser: Zero-index-materials laser," *IEEE Journal on Multiscale and Multiphysics Computational Techniques*, Vol. 4, 133–142, 2019.
17. Liao, S. and L. Ou, "High-Q interstitial square coupled microring resonators arrays," *IEEE Journal of Quantum Electronics*, Vol. 56, No. 4, 1–8, August 2020.
18. Liao, S., T. Wong, Z. Wang, R. Wang, E. Clutter, and H.-T. Chien, "Miniature fiber laser microphones with graphene diaphragms," *2018 IEEE Research and Applications of Photonics In Defense Conference (RAPID)*, 1–4, August 2018.
19. Peng, Y. and S. Liao, "On-chip ZIM-BiC laser," *2019 IEEE MTT-S International Conference on Numerical Electromagnetic and Multiphysics Modeling and Optimization (NEMO)*, 1–4, May 2019.
20. Zeng, Y., Z. Tang, S. Liao, and Y. Peng, "Integrated photonics devices using zeroindex metamaterials," *2019 Photonics & Electromagnetics Research Symposium —Fall (PIERS — Fall)*, 1458–1460, December 2019.
21. El-Ganainy, R., K. G. Makris, D. N. Christodoulides, and Z. H. Musslimani, "Theory of coupled optical PT-symmetric structures," *Optics Letters*, Vol. 32, No. 17, 2632–2634, September 2007.
22. Makris, K. G., R. El-Ganainy, D. N. Christodoulides, and Z. H. Musslimani, "Beam dynamics in PT symmetric optical lattices," *Physical Review Letters*, Vol. 100, No. 10, 103904, March 2008.
23. Musslimani, Z. H., K. G. Makris, R. El-Ganainy, and D. N. Christodoulides, "Optical solitons in PT periodic potentials," *Physical Review Letters*, Vol. 100, No. 3, 030402, January 2008.
24. Ruschhaupt, A., F. Delgado, and J. G. Muga, "Physical realization of PT-symmetric potential scattering in a planar slab waveguide," *Journal of Physics A: Mathematical and General*, Vol. 38, No. 9, L171–L176, February 2005.
25. Klaiman, S., U. Günther, and N. Moiseyev, "Visualization of Branch Points in PT-symmetric waveguides," *Physical Review Letters*, Vol. 101, No. 8, 080402, August 2008.
26. Longhi, S., "Time reversal of a discrete system coupled to a continuum based on non-Hermitian IP," *Science Bulletin*, Vol. 62, No. 12, 869–874, June 2017.
27. Rodríguez-Lara, B. M., R. El-Ganainy, and J. Guerrero, "Symmetry in optics and photonics: A group theory approach," *Science Bulletin*, Vol. 63, No. 4, 244–251, February 2018.
28. Hodaei, H., M.-A. Miri, M. Heinrich, D. N. Christodoulides, and M. Khajavikhan, "Parity-time-symmetric microring lasers," *Science*, Vol. 346, No. 6212, 975–978, November 2014.
29. Savoia, S., G. Castaldi, V. Galdi, A. Alù, and N. Engheta, "PT symmetry-induced wave confinement and guiding in ϵ-near-zero metamaterials," *Physical Review B*, Vol. 91, No. 11, 115114, March 2015.
30. Liao, S. and R. J. Vernon, "On the image approximation for electromagnetic wave propagation and PEC scattering in cylindrical harmonics," *Progress In Electromagnetics Research*, Vol. 66, 65–88, 2006.
31. Liao, S. and R. J. Vernon, "The near-field and far-field properties of the cylindrical modal expansions with application in the image theorem," *2006 Joint 31st International Conference on Infrared Millimeter Waves and 14th International Conference on Teraherz Electronics*, 260–260, September 2006.
32. Liao, S. and R. J. Vernon, "A new fast algorithm for calculating near-field propagation between arbitrary smooth surfaces," *2005 Joint 30th International Conference on Infrared and Millimeter Waves and 13th International Conference on Terahertz Electronics*, Vol. 2, 606–607, September 2005.
33. Liao, S., H. Soekmadji, and R. J. Vernon, "On fast computation of electromagnetic wave propagation through FFT," *2006 7th International Symposium on Antennas, Propagation EM Theory*, 1–4, October 2006.
34. Liao, S. and R. J. Vernon, "The cylindrical Taylor-interpolation FFT algorithm," *2006 Joint 31st International Conference on Infrared Millimeter Waves and 14th International Conference on Teraherz Electronics*, 259–259, September 2006.

35. Liao, S., "Beam-shaping PEC mirror phase corrector design," *PIERS Online*, Vol. 3, No. 4, 392–396, 2007.
36. Liao, S., "Fast computation of electromagnetic wave propagation and scattering for quasicylindrical geometry," *PIERS Online*, Vol. 3, No. 1, 96–100, 2007.
37. Liao, S., "On the validity of physical optics for narrow-band beam scattering and diffraction from the open cylindrical surface," *PIERS Online*, Vol. 3, No. 2, 158–162, 2007.
38. Liao, S., R. J. Vernon, and J. Neilson, "A high-efficiency four-frequency mode converter design with small output angle variation for a step-tunable gyrotron," *2008 33rd International Conference on Infrared, Millimeter and Terahertz Waves*, 1–2, September 2008.
39. Liao, S., R. J. Vernon, and J. Neilson, "A four-frequency mode converter with small output angle variation for a step-tunable gyrotron," *Electron Cyclotron Emission and Electron Cyclotron Resonance Heating (EC-15)*, 477–482, World Scientific, April 2009.
40. Vernon, R. J., "High-power microwave transmission and mode conversion program," *Technical Report DOEUW52122*, Univ. of Wisconsin, Madison, WI (United States), August 2015.
41. Liao, S., "Multi-frequency beam-shaping mirror system design for high-power gyrotrons: Theory, algorithms and methods," Ph.D. Thesis, University of Wisconsin at Madison, USA, 2008.
42. Liao, S. and R. J. Vernon, "A fast algorithm for wave propagation from a plane or a cylindrical surface," *International Journal of Infrared and Millimeter Waves*, Vol. 28, No. 6, 479–490, June 2007.
43. Liao, S.-L. and R. J. Vernon, "Sub-THz beam-shaping mirror system designs for quasi-optical mode converters in high-power gyrotrons," *Journal of Electromagnetic Waves and Applications*, Vol. 21, No. 4, 425–439, Taylor & Francis, January 2007.
44. Liao, S., "Miter bend mirror design for corrugated waveguides," *Progress In Electromagnetics Research*, Vol. 10, 157–162, EMW Publishing, 2009.
45. Liao, S. and R. J. Vernon, "A fast algorithm for computation of electromagnetic wave propagation in half-space," *IEEE Transactions on Antennas and Propagation*, Vol. 57, No. 7, 2068–2075, July 2009.
46. Liao, S., N. Gopalsami, A. Venugopal, A. Heifetz, and A. C. Raptis, "An efficient iterative algorithm for computation of scattering from dielectric objects," *Optics Express*, Vol. 19, No. 4, 3304–3315, Optical Society of America, February 2011.
47. Liao, S., "Spectral-domain MOM for planar meta-materials of arbitrary aperture waveguide array," *2019 IEEE MTT-S International Conference on Numerical Electromagnetic and Multiphysics Modeling and Optimization (NEMO)*, 1–4, May 2019.
48. Schindler, J., A. Li, M. C. Zheng, F. M. Ellis, and T. Kottos, "Experimental study of active LRC circuits with PT-symmetries," *Physical Review A*, Vol. 84, No. 4, 040101, October 2011.
49. Schindler, J., Z. Lin, J. M. Lee, H. Ramezani, F. M. Ellis, and T. Kottos, "PT-symmetric electronics," *Journal of Physics A: Mathematical and Theoretical*, Vol. 45, No. 44, 444029, October 2012.
50. Ra'di, Y., D. L. Sounas, A. Alù, and S. A. Tretyakov, "Parity-time-symmetric teleportation," *Physical Review B*, Vol. 93, No. 23, 235427, June 2016.
51. Chen, P.-Y., M. Sakhdari, M. Hajizadegan, Q. Cui, M. M.-C. Cheng, R. El-Ganainy, and A. Alù, "Generalized parity-time symmetry condition for enhanced sensor telemetry," *Nature Electronics*, Vol. 1, No. 5, 297–304, May 2018.
52. Zhu, L., N. Alkhaldi, H. M. Kadry, S. Liao, and P.-Y. Chen, "A compact hybrid-fed microstrip antenna for harmonics-based radar and sensor systems," *IEEE Antennas and Wireless Propagation Letters*, Vol. 17, No. 12, 2444–2448, December 2018.
53. Padmaraj, S., K. Nirish Patil, and S. Liao, "A compact dual-band WiFi energy harvester," *2019 Photonics & Electromagnetics Research Symposium — Fall (PIERS — Fall)*, 1209–1212, Xiamen, China, December 17–20, 2019.